

# Noncentrosymmetric Structure from a Tetrablock Quarterpolymer of the ABCA Type

A. Takano,<sup>\*,†</sup> K. Soga,<sup>†</sup> J. Suzuki,<sup>‡</sup> and Y. Matsushita<sup>†</sup>

Department of Applied Chemistry, Nagoya University, Furo-cho, Chikusa-ku, Nagoya 464-8603, Japan, and The Computing Research Center, High Energy Accelerator, Research Organization, 1-1 Oho, Tsukuba 305-0801, Japan

Received September 10, 2003

Revised Manuscript Received October 16, 2003

Nanoscopic crystal without a crystallographic symmetry plane could be a novel nanoscale nonlinear optical material since it should show high polarizability because of its dipole moment. It is established that block and graft copolymers show microphase-separated structure with nanoscopic periodicity of the order of 10–100 nm due to intramolecular phase separation among component polymers.<sup>1–3</sup> Linear two- and three-component block copolymers are known in general to show a centrosymmetric microdomain structure, owing to the head-to-head or tail-to-tail assembly manner of asymmetric or symmetric molecules. The former consists of AB-type diblock copolymers,<sup>2–4</sup> ABA-type triblock copolymers,<sup>5</sup> and (AB)<sub>n</sub> star-branched copolymers,<sup>6</sup> while ABC-type<sup>7–9</sup> triblock copolymers belong to the latter. On the other hand, Goldacker et al. found noncentrosymmetric structure as a part of the whole microphase-separated region for the ABC/AC block copolymer blend system,<sup>10</sup> where the repeating unit of the microdomain structure is –ABC–, while Wickham and Shi reported on the phase behavior of the same blend system by numerical calculation using self-consistent mean-field theory.<sup>11</sup> Furthermore, noncentrosymmetric structure has been reported for the ferroelectric property using an ABCA molecule.<sup>12</sup>

One-way alignment of asymmetric macromolecules containing more than three components has to be realized to obtain nanoscopic self-assembled structures without symmetry planes. Apparently, successful results cannot be obtained from the pure ABC system as stated above; therefore, we selected a tetrablock copolymer of the ABCA type instead. There are two possibilities to align ABCA tetrablock molecules into three phases. They are compared schematically in Figure 1, assuming lamellar structure. Figure 1a expresses assembly of one-way alignment of the ABCA molecule, where the repeating unit of microdomains is simply –ABC–, while Figure 1c stands for the well-known two-way arrangement of the same molecule, where the repeating unit is two molecular lengths and so the force should be –ABCACB–. The coexistence of two polymer orientations in a single microdomain must be forbidden in the strong segregation regime where B and C component polymers strongly repel each other. Alternatively, however, it is quite possible for this polymer system to adopt two different assembly manners simul-

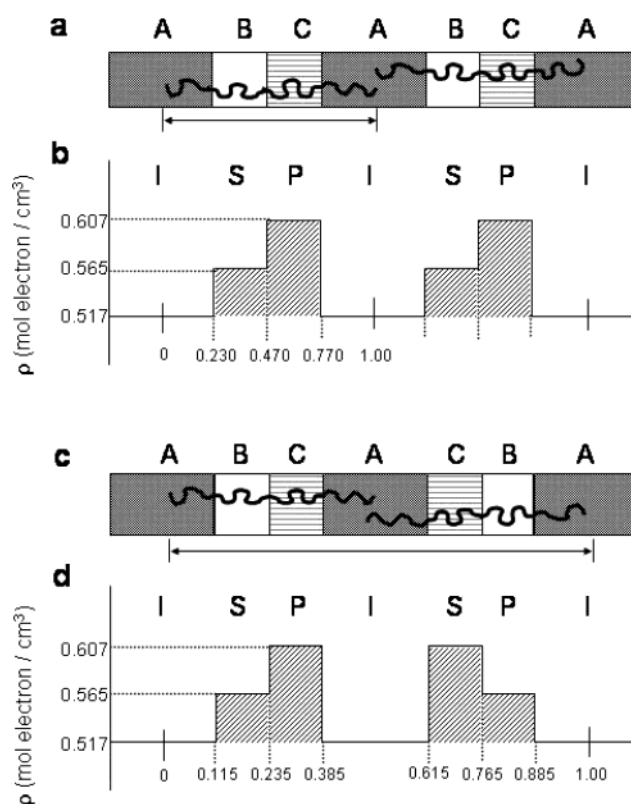


**Figure 1.** Schematic comparison of noncentrosymmetric lamellar microdomain order and centrosymmetric one. (a) One-way aligned manner of ABCA molecules in microdomain structure. The repeating unit should be –A–B–C–, which corresponds to –I–S–P– for our present tetrablock quarterpolymer. The darkness of each microdomain represents very simplified TEM contrast. Osmium tetroxide heavily stains the I phase, moderately does the P phase, and very lightly does the S phase. (b) Electron density profile corresponding to (a). The crystallographic unit cell can be chosen as –(I/2)–S–P–(I/2)– so that several Bragg's peaks come from this one-dimensional "crystal". This profile includes actually two-step stairs which behaves as the isolated asymmetric microdomain in matrix. (c) Two-way aligned manner of the ABCA molecules, where the repeating unit is –A–B–C–A–C–B–, that is –I–S–P–I–P–S– for the present sample. (d) Electron density profile corresponding to (c). Crystallographic unit cell chosen here is –I/2–S–P–I–P–S–I/2–.

taneously as the result of macroscopic phase separation behavior between one-way aligned and two-way aligned grains with certain small sizes.

A monodisperse block copolymer sample in both molecular weight and composition was prepared under vacuum by anionic polymerizations of two kinds of diblock copolymers, i.e., poly(isoprene-*block*-styrene) (IS) and poly(isoprene-*block*-2-vinylpyridine) (IP), the former being an end-functionalized polymer with a diphenylethylene group whereas the latter is the carbanion living polymer with an active site on a chain end of poly(2-vinylpyridine), followed by coupling between them to produce the IS–PI molecule.<sup>13</sup> The tetrablock quarterpolymer was isolated from the crude as-polymerized polymer mixture by size-exclusion chromatography (SEC) fractionation using a HPLC system of TOSOH Co. The total number-averaged molecular weight measured by using a membrane osmometer of Hewlett-Packard in toluene at 303 K was  $1.32 \times 10^5$  with a very

<sup>†</sup> Nagoya University.

<sup>‡</sup> High Energy Accelerator, Research Organization.

\* To whom correspondence should be addressed.

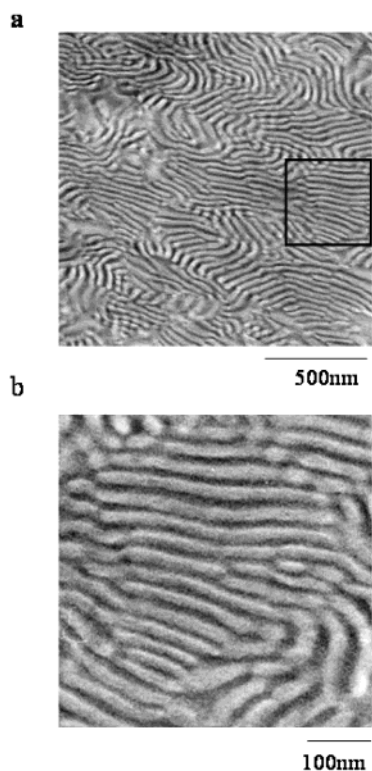


**Figure 2.** Bright field transmission electron micrographs obtained from an ISPI tetrablock quarterpolymer. The thickness of the ultrathin section is about 50 nm. (a) Low-magnification image viewing many small grains. The size of each grain is apparently much smaller than those of the well-studied block copolymers, which normally exceeds 10  $\mu\text{m}$ . (b) High-magnification image showing lamellar arrangement. The repeating unit mostly consists of -black-white-gray- stripes which corresponds to -I-S-P- phases.

low apparent molecular weight distribution of 1.02 determined by an analytical SEC of TOSOH. Volume fractions of four blocks determined by a 500 MHz  $^1\text{H}$  NMR of Varian were 0.23, 0.24, 0.30, and 0.23. The sample film was obtained by solvent casting from a dilute solution of tetrahydrofuran and dried well under vacuum followed by annealing at 150  $^\circ\text{C}$  for 24 h. Bulk structure of the film specimen was observed by two different methods, i.e., transmission electron microscopy (TEM) and small-angle X-ray scattering (SAXS) used compensatively. The film was stained with osmium tetroxide and cut into ultrathin sections with thickness of ca. 50 nm by an ultramicrotome, Ultracut UCT of LEICA, and their microphase-separated structures were observed by a transmission electron microscope, H-800 of Hitachi, under an acceleration voltage of 100 kV.

Figure 2 shows bright field transmission electron micrographs at different magnifications of an ultrathin section of the quarterpolymer observed from the edge view of the cast film. Figure 2a reveals that lamellar structure with three-step magnitude of the contrast is apparently formed by this tetrablock quarterpolymer covering almost all the region of the micrograph, though its grain size is quite small below 1  $\mu\text{m}$ . Figure 2b is an enlarged image of a part of that in Figure 2a; its repeating unit with length of about 35 nm includes three stripes arrayed in the order of black-white-gray, which corresponds to I, S, and P phases since the ultrathin section was stained with osmium tetroxide.<sup>7</sup> This is schematically represented in Figure 1, where the correspondence of block quarterpolymer chains to indi-

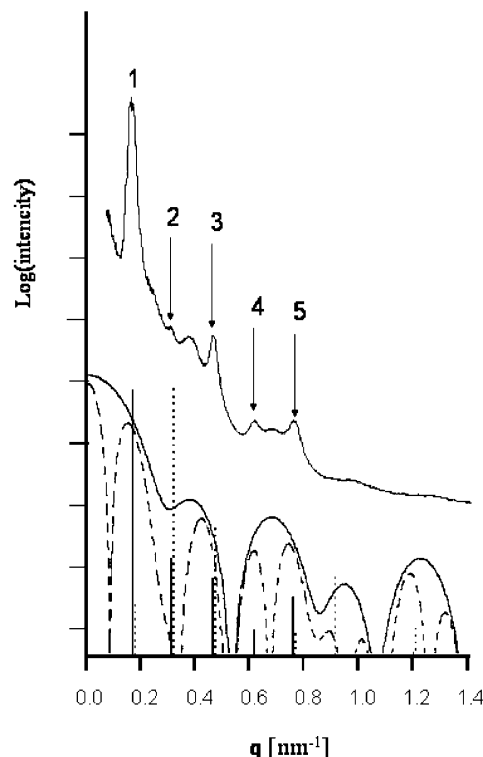


**Figure 3.** Small-angle X-ray scattering diffraction pattern of the ISPI tetrablock quarterpolymer. Sample geometry is the edge view where incident X-rays are parallel to the film surface. Vertical thick bars at the lower section denote calculated diffracted intensities based on the noncentrosymmetric periodic structure shown in Figure 1b, while the solid curve expresses "domain" scattering calculated by using the profile of two-step stairs as also shown in the same figure (Appendix). The vertical dotted bars represent calculated intensities based on centrosymmetric structure shown in (d), while the dotted curve is the "domain" scattering for a symmetric profile in the same figure.

vidual domains is shown assuming the cross section of lamellar structure. One notices from Figure 1a that this structure has no symmetry plane along the direction parallel to the domain interface. This fact suggests that one-way alignment of the pure quarterpolymer molecule has been achieved; that is, it gives noncentrosymmetric material with nanoscopic scale length as expected.

On the other hand, Figure 3 shows a small-angle X-ray scattering pattern for the same film sample. Several diffraction peaks originating from lamellar structure are clearly observed. Vertical thick bars in Figure 3 are the calculated relative peak heights using the very simplified electron density profile in Figure 1b (Appendix). The locations and the heights, which are actually the magnitude of the calculated diffraction intensities expressing the squares of the structure factors at each diffraction plane up to higher order, agree well with the diffracted peaks observed and numbered with an integer which appears very regularly along with horizontal axis, being the magnitude of the scattering vector  $|q|$  ( $= 4\pi \sin \theta/\lambda$ ), where  $2\theta$  is the scattering angle and  $\lambda$  denotes the wavelength of X-rays. Furthermore, underneath the observed intensity curve, the solid curve shows the "particle" scattering function which was calculated using the asymmetric electron density profile for actually two-step stairs corresponding to S and P phases in the matrix of the I phase as one can easily recognize as hatched portions in Figure 1c (Appendix). Comparing the observed and the calculated

intensity curves, we notice that several diffracted peaks can be explained by this "particle" scattering function. They are a relatively broad shoulder appearing between peaks 1 and 2 and the broad peaks appearing between peaks 2 and 3 at  $q = 0.38 \text{ nm}^{-1}$  and also between peaks 4 and 5 at  $q = 0.67 \text{ nm}^{-1}$  and two more at higher  $q$  region at around  $0.94$  and  $1.24 \text{ nm}^{-1}$ , respectively. As a result, all the peaks in the observed scattering curve can be explained quite consistently by a combination of the calculated diffracted intensities having two mutually correlated but different origins mentioned above.

Applying the same method, intensities for the centrosymmetric structure were calculated using the electron density profile in Figure 1d. The calculated relative intensities corresponding to the lamellar repeating structure are shown in Figure 3 as vertical dotted bars beside each solid bar, while the particle scattering factor is drawn as a dotted line also at the bottom of Figure 3. Obviously this diffracted pattern contradicts the observed one.

The repeating distance estimated by applying the magnitudes of the indexed peaks to Bragg's condition is  $41 \text{ nm}$ , which is consistent with the microdomain size observed by TEM. Further very interestingly this value is equivalent and even smaller than the domain size,  $48 \text{ nm}$ , for the IP diblock copolymer which is one of the two precursors obtained in the course of preparing ISPI tetrablock quarterpolymer. This can be explained by considering that the repeating distance of IP diblock copolymer corresponds to two molecular lengths as a result of the two-way alignment nature of the diblock copolymer molecule, while the repeating distance for ISPI could be one molecular length as shown in Figure 1a. This is another definite evidence of the one-way arrangement of this tetrablock quarterpolymer resulting in forming asymmetric structure. These experimental results from X-rays ensure that the noncentrosymmetric structure covers almost the whole sample region, since the beam size of X-rays,  $0.7 \text{ mm} \times 0.5 \text{ mm}$ , is much larger than grain size. This feature should have advantages for engineering purposes.

From these facts, we conclude that the ISPI tetrablock quarterpolymer of the ABCA type can be self-assembled to form a noncentrosymmetric structure though the long-distance ordering is less than the regular centrosymmetric structures. This deficiency needs to be overcome so as to extend this result to several applications in the future.

**Acknowledgment.** This work was partially supported by the Ministry of Education, Science, Sports and Culture, Grant-in-Aid program #12450383 and #13031040. This research was supported in part by a grant from Daiko Foundation. The authors thank them for their financial assistance. The authors greatly thank Mr. S. Arai at the Center for Integrated Research in Science and Engineering in Nagoya University for his help in taking transmission electron micrographs.

**Appendix.** In small-angle X-ray scattering experiments for the present sample in microphase-separated bulk, the diffracted scattering intensity  $I(\mathbf{q})$  is associated with two components, the structure factor  $S(\mathbf{q})$  and form factor  $F(\mathbf{q})$ , according to the following equation:

$$I(\mathbf{q}) \propto |S(\mathbf{q}) * F(\mathbf{q})|^2 \quad (1)$$

In eq 1,  $S(\mathbf{q})$  denotes electron density at vector  $\mathbf{r}$  from

the origin of a unit cell, which actually gives diffracted intensities based on crystallographic repeating unit, while form factor  $F(\mathbf{q})$  is actually domain scattering from each "domain" embedded in matrix polymer. Since scattering intensity can be represented by Fourier transform of electron density

$$|S(\mathbf{q}) * F(\mathbf{q})|^2 = \left| \int \rho(\mathbf{r}) \exp(i\mathbf{q}\mathbf{r}) d\mathbf{r} \right|^2 \quad (2)$$

where  $\rho(\mathbf{r})$  denotes the electron density at vector  $\mathbf{r}$  from the origin of a unit cell of the lattice. Equation 2 can be rewritten by using sine and cosine functions as follows:

$$\begin{aligned} I(\mathbf{q}) &\propto \left| \int \rho(\mathbf{r}) \exp(i\mathbf{q}\mathbf{r}) d\mathbf{r} \right|^2 = \\ &\quad \left| \int \rho(r) [\cos(\mathbf{q}\mathbf{r}) + i \sin(\mathbf{q}\mathbf{r})] d\mathbf{r} \right|^2 \\ &= \left| \int \rho(r) \cos(\mathbf{q}\mathbf{r}) d\mathbf{r} + i \int \rho(r) \sin(\mathbf{q}\mathbf{r}) d\mathbf{r} \right|^2 \\ &= \left[ \int \rho(r) \cos(qr) dr \right]^2 + \left[ \int \rho(r) \sin(qr) dr \right]^2 \quad (3) \end{aligned}$$

Lamellar structure can be regarded as one-dimensional lattice; therefore, the scattering intensity  $I(\mathbf{q})$  can be calculated using scalar quantity  $q$  and  $r$ , instead of  $\mathbf{q}$  and  $\mathbf{r}$ . Thus,  $I(\mathbf{q})$  is replaced by  $I(q)$  hereafter. As for structure factor  $S(q)$ , intensities at discrete values,  $|q|_{h00}$ , associate with  $[h00]$  diffracted planes are essentially meaningful, where  $h$  is the Miller index. Using this notation, the structure factor component can be written as

$$S(q) \propto \left[ \int_0^1 \rho(r) \cos(|q|_{h00} r) dr \right]^2 + \left[ \int_0^1 \rho(r) \sin(|q|_{h00} r) dr \right]^2 \quad (4)$$

$S(q)$  for the noncentrosymmetric lamellar structure can be calculated using electron densities and volume fractions of a three-component ISPI tetrablock quarterpolymer shown in Figure 1b according to eq 4.

$$\begin{aligned} S(q) &\propto \left[ \int_0^{0.230} 0.517 \cos(|q|_{h00} r) dr + \right. \\ &\quad \left. \int_{0.230}^{0.470} 0.565 \cos(|q|_{h00} r) dr + \right. \\ &\quad \left. \int_{0.470}^{0.770} 0.608 \cos(|q|_{h00} r) dr + \right. \\ &\quad \left. \int_{0.770}^{1.00} 0.517 \cos(|q|_{h00} r) dr \right]^2 + \\ &\quad \left[ \int_0^{0.230} 0.517 \sin(|q|_{h00} r) dr + \right. \\ &\quad \left. \int_{0.230}^{0.470} 0.565 \sin(|q|_{h00} r) dr + \right. \\ &\quad \left. \int_{0.470}^{0.770} 0.608 \sin(|q|_{h00} r) dr + \int_{0.770}^{1.00} 0.517 \sin(|q|_{h00} r) dr \right]^2 \quad (5) \end{aligned}$$

$S(q)$ s were actually calculated for each index  $h = 1, 2, 3$ , etc., using the cell size  $d_{100} = 41 \text{ nm}$  and the relationship  $|q| = 2\pi/d_{100}$ , and they are drawn in Figure 3 as solid vertical bars.

On the other hand,  $F(q)$  can be calculated using electron density differences and volume fractions of the

S and P phase embedded in the I matrix shown in hatched portions in Figure 1b according to eq 6.

$$\begin{aligned}
 F(q) \propto & \left[ \int_0^{0.230} (0.517 - 0.517) \cos(\mathbf{q}r) \, dr + \right. \\
 & \int_{0.230}^{0.470} (0.565 - 0.517) \cos(\mathbf{q}r) \, dr + \\
 & \int_{0.470}^{0.770} (0.608 - 0.517) \cos(\mathbf{q}r) \, dr + \\
 & \left. \int_{0.770}^{1.00} (0.517 - 0.517) - \cos(\mathbf{q}r) \, dr \right]^2 + \\
 & \left[ \int_0^{0.230} (0.517 - 0.517) \sin(\mathbf{q}r) \, dr + \right. \\
 & \int_{0.230}^{0.470} (0.565 - 0.517) \sin(\mathbf{q}r) \, dr + \\
 & \left. \int_{0.470}^{0.770} (0.608 - 0.517) \sin(\mathbf{q}r) \, dr + \right. \\
 & \left. \int_{0.770}^{1.00} (0.517 - 0.517) \sin(\mathbf{q}r) \, dr \right]^2 \\
 = & \left[ \int_{0.230}^{0.470} 0.048 \cos(\mathbf{q}r) \, dr + \int_{0.470}^{0.770} 0.091 \cos(\mathbf{q}r) \, dr \right]^2 + \\
 & \left[ \int_{0.230}^{0.470} 0.048 \sin(\mathbf{q}r) \, dr + \int_{0.470}^{0.770} 0.091 \sin(\mathbf{q}r) \, dr \right]^2 \quad (6)
 \end{aligned}$$

The results are shown as a solid line in Figure 3.

## References and Notes

- (1) Molau, G. E. In *Block Copolymers*; Aggarwal, S. L., Ed.; Plenum Press: New York, 1970; pp 79–106.
- (2) Leibler, L. *Macromolecules* **1980**, *13*, 1602–1617.
- (3) Bates, F. S.; Fredrickson, G. H. *Annu. Rev. Phys. Chem.* **1990**, *41*, 525–557.
- (4) Helfand, E.; Tagami, Y. *J. Chem. Phys.* **1972**, *56*, 3592–3360.
- (5) Matsushita, Y.; Nomura, M.; Watanabe, J.; Mogi, Y.; Noda, I. *Macromolecules* **1995**, *28*, 6007–6013.
- (6) Thomas, E. L.; Anderson, D. M.; Henkee, C. S.; Hoffman, D. *Nature (London)* **1988**, *334*, 598–601.
- (7) Mogi, Y.; Nomura, M.; Kotsuji, H.; Ohnishi, K.; Matsushita, Y.; Noda, I. *Macromolecules* **1994**, *27*, 6755–6760.
- (8) Stadler, R.; Auschra, C.; Beckmann, J.; Krappe, U.; Voight-Martin, I.; Leibler, L. *Macromolecules* **1995**, *28*, 3080–3097.
- (9) Matsen, M. W. *J. Chem. Phys.* **1998**, *108*, 785.
- (10) Goldacker, T.; Abetz, V.; Stadler, R.; Erukhimovich, I.; Leibler, L. *Nature (London)* **1999**, *398*, 137–139.
- (11) Wickham, R. A.; Shi, A.-C. *Macromolecules* **2001**, *34*, 6487–6494.
- (12) Petschek, R. G.; Wiefeling, K. M. *Phys. Rev. Lett.* **1987**, *59*, 343–346.
- (13) Takano, A.; Kadoi, O.; Hirahara, K.; Kawahara, S.; Isono, Y.; Suzuki, J.; Matsushita, Y. *Macromolecules* **2003**, *36*, 3045–3050.

MA035344Z